Available online at www.sciencedirect.com
SCIENCE DIRECT
Biochemical and Biophysical Research Communications 345 (2006) 59–66
BBRC
www.elsevier.com/locate/ybbrc

Slow-inactivation induced conformational change in domain 2-segment 6 of cardiac Na^+ channel

John P. O'Reilly *, Penny E. Shockett

Department of Biological Sciences SLU 10736, Southeastern Louisiana University, Hammond, LA 70402, USA

Received 9 April 2006
Available online 25 April 2006

Abstract

To examine conformational changes during slow inactivation involving domain 2-segment 6 (D2-S6) of human cardiac Na^+ channel (hNav1.5), we applied the substituted-cysteine accessibility method (SCAM) using methanethiosulfonate ethylammonium (MTSEA). We substituted cysteine (C) for native valine (V) at position 930 of D2-S6 in the MTSEA-resistant hNav1.5 mutant C373Y to produce the double mutant C373Y-V930C. Whole-cell Na^+ currents were recorded using patch-clamp techniques in transiently transfected HEK cells. In C373Y-V930C, we find that MTSEA (1.5 mM) applied in the closed state (−160 mV) has no significant effect on whole-cell Na^+ current, while MTSEA applied in the slow-inactivated state (prolonged depolarization at 0 mV) decreases current. We propose that D2-S6 in hNav1.5 undergoes molecular rearrangement during slow inactivation exposing the side chain of residue 930 such that it becomes accessible to modification by MTSEA.

Keywords: Na^+ channels; Site-directed mutagenesis; D2-S6; hNav1.5; Methanethiosulfonate (MTS); Slow inactivation

Voltage-gated Na^+ channels (Navs) are transmembrane proteins, the main component of which is an α-subunit consisting of four homologous domains (D1–D4), each with six transmembrane segments (S1–S6). Although several Nav isoforms are associated with modulatory accessory β-subunits, the α-subunit is capable of channel function, i.e., voltage-sensitivity, activation, ion selectivity, and inactivation, when expressed alone in heterologous expression systems such as *Xenopus oocytes* and mammalian HEK cells [1–3].

Navs respond rapidly to depolarization of the membrane, allowing Na^+ ions, driven by their electrochemical gradient, to cross the membrane via an intraprotein permeation pore. This process, termed activation, is responsible for the initiation and propagation of action potentials in most excitable tissues such as those comprising the nervous system, cardiac muscle, and skeletal muscle. In response to the same stimulus (i.e., depolarization) Navs enter a non-conducting state called inactivation from which they rarely activate. This process is observed to occur over two different time scales. One type of inactivation occurs within milliseconds of depolarization and is appropriately termed fast inactivation. This inactivation is important for the termination of action potentials [4]. The other type of inactivation, which occurs with prolonged depolarizations (seconds to minutes), is called slow inactivation and likely plays a role in membrane excitability and action potential firing patterns [5,6]. In addition to differences between the kinetics of fast and slow inactivation, these processes involve different molecular mechanisms. For example, fast inactivation can be eliminated by internal perfusion of protease or amino acid substitutions in the D3–D4 linker (the fast inactivation "gate"), manipulations that do not eliminate slow inactivation [7,8].

Because electrophysiological function of Navs is critically dependent on molecular structure, it is not surprising that amino acid alterations in Navs can disrupt normal function of excitable tissues. Nearly twenty human disease states have been attributed to heritable mutations in Navs

* Corresponding author. Fax: +1 985 549 3810.
E-mail address: joreilly@selu.edu (J.P. O'Reilly).

0006-291X/$ - see front matter © 2006 Elsevier Inc. All rights reserved.
doi:10.1016/j.bbrc.2006.04.049

or "channelopathies" [9]. For example, more than 150 mutations in neuronal Navs have been identified in patients with epilepsy [10], more than 25 mutations in skeletal muscle Navs have been found that produce myotonias [11], and at least five mutations in human heart Navs are found in patients with long QT syndrome and Brugada's syndrome [12]. Many of these mutant Navs have been studied in heterologous expression systems such as *Xenopus oocytes* and HEK cells, and diverse effects caused by the mutations on activation, fast inactivation, and/or slow inactivation have been described [13].

Understanding the relationship between molecular structure and physiological function has been greatly aided by the cloning and expression of Navs. For example, activation is dependent on the voltage-sensing S4 segments [14], and the cytoplasmic linker between D3 and D4 appears to be the fast-inactivation gate or hinge [15]. However, the molecular events occurring during slow inactivation are not well defined. One hypothesis poses that during slow inactivation of Navs, the outer mouth of the pore collapses, a mechanism similar to C-type inactivation of K^+ channels [16]. A second hypothesis involves a rearrangement of amino acid residues within the putative pore-lining S6 segments [17] that would constrict the inner pore region [18]. In support of the latter hypothesis are studies showing that mutations in S6 have effects on slow-inactivation gating [18–21].

In the present study, we substituted cysteine (C) for native valine (V) at the inner pore residue 930 (V930C) in D2-S6 of the human cardiac muscle Nav hNav1.5. We chose this residue in hNav1.5 because we previously found state-dependent molecular rearrangement at the homologous site (V787 in D2-S6) in rat skeletal muscle rNav1.4 [18]. We were interested in determining if Nav1.5 and Nav1.4 isoforms share similar molecular mechanisms of slow inactivation despite the fact that Nav1.5 is relatively resistant to slow inactivation compared with Nav1.4 [22,23].

In an effort to detect conformational changes in D2-S6 during slow inactivation in hNav1.5, we used methanethiosulfonate ethylammonium (MTSEA) and the substituted-cysteine accessibility method (SCAM) [24]. We found that application of MTSEA to wild-type hNav1.5 rapidly reduces current, an effect that is also found in the rat cardiac Na^+ channel rNav1.5 [25]. Therefore, we studied the V930C mutant in the MTSEA-resistant hNav1.5 mutant C373Y background (C373Y-V930C). Our data extend previous studies and support the hypothesis that D2-S6 in hNav1.5 undergoes conformational change during slow inactivation enhancing MTSEA-accessibility at residue 930.

Materials and methods

Site-directed mutagenesis. Nav mutagenesis was carried out using an adapted 2-stage modification of the Quick Change XL Site Directed Mutagenesis Kit Protocol (Stratagene, La Jolla, CA, USA, and personal communication, Sho-Ya Wang, SUNY Albany, NY, USA) [26,27]. pcDNA1 (Invitrogen, Carlsbad, CA, USA) containing hNav1.5 cDNA was used as the template for mutagenesis. For each mutation, a mutagenesis mix (Stratagene, La Jolla, CA, USA) was prepared containing 74 ng of template plasmid, 2.1% dNTP mix, 6.3% QuickSolution, 10.5% of 10× Reaction Buffer, and 1.5 U *PfuTurbo* DNA polymerase in a final volume of 28 μl. 13.3 μl mix was added to each of two 200 μl thin-walled PCR tubes. Seventy nanograms of top strand mutagenic oligonucleotide was added to one tube containing mix (Stage 1, 14 μl total volume) and 70 ng lower strand mutagenic oligonucleotide was added to the other tube containing mix (Stage 2, 14 μl total volume). For Stage 1 reaction, PCR was carried out as follows: Step 1, 94 °C, 30 s; Step 2, 94 °C, 30 s; Step 3, 55 °C, 1 min; Step 4, 68 °C, 23 min; followed by Step 5, 3 cycles to Step 2. Stage 1 reaction product was then combined with Stage 2 tube (28 μl total combined volume), an additional 0.5 U *PfuTurbo* DNA polymerase was added, and mixture subjected to Stage 2 PCR as follows: Step 1, 94 °C, 30 s; Step 2, 94 °C, 30 s; Step 3, 55 °C, 1 min; Step 4, 68 °C, 23 min; Step 5, 17 cycles to Step 2; Step 6, 68 °C, 7 min. Ten microliters of product was digested for 1 h at 37 °C with 2 U *Dpn*I, digestion was repeated, and product transformed into XL10-Gold as recommended by the supplier (Stratagene, La Jolla, CA, USA). Colonies growing on LB-ampicillin plates were picked, grown in LB containing 50 μg/ml ampicillin, and plasmid DNA isolated using a Wizard Plus SV miniprep kit (Promega, Madison, WI, USA). Plasmid DNA was digested with *Eco*RI to check overall integrity, sequenced on both strands in regions encompassing putative mutations (Pennington Biomedical Genomics Core Facility, Baton Rouge, LA, USA), and intact clones containing mutations selected for study. Plasmid DNA for transfection was purified using maxi prep columns (Qiagen, Valencia, CA, USA). Oligonucleotides for mutagenesis included; hH1-C373Y-top CGCCTGATGACGCAGGACTACTGGG AGCGCCTCTATCAG, hH1-C373Y-bot CTGATAGAGGCGCTCCC AGTAGTCCTGCGTCATCAGGCG, hH1-V930C-top GTCATTGGC AACCTTGTGTGCCTGAATCTCTTCCTGGCC, hH1-V930C-bot GG CCAGGAAGAGATTCAGGCACACAAGGTTGCCAATGAC. DNA sequencing primers included; hH1C373Y-seqfor CTGTGTGGGAACAG CTCTGAC, hH1C373Y-seqrev GTAGAAGGACCCCAGGAAGATG, (D2-S6)mut-seqfor CCTAATCATCTTCCGCATCC, and (D2-S6)mut-seqrev GGAGACCACAGCAGAAATCC. All oligonucleotides were obtained commercially (Operon Biotechnologies, Huntsville, AL, USA).

Transient transfection. Plasmid expression constructs containing wild-type and mutant Nav cDNA clones were transiently transfected into HEK cells using calcium phosphate precipitation as previously described [22,28]. The transfection included 1–5 μg of a plasmid encoding cell surface antigen CD8 (OriGene, Rockville, MD, USA) and 5–10 μg of Nav cDNA expressed from pcDNA1 (Invitrogen, Carlsbad, CA, USA).

Electrophysiology. Using standard patch-clamp techniques [29], we recorded whole-cell peak Na^+ current (I_{Na}) from transiently transfected HEK cells. Recordings were performed at room temperature (21–22 °C), without correction for liquid junction potential. Activation (conductance–voltage) and steady-state fast inactivation (h_∞) curves were obtained approximately 5 min after rupture of the membrane. Recording micropipettes (Drummond Scientific, Broomall, PA, USA) were pulled on a Model P-97 Flaming-Brown puller (Sutter Instruments, Novato, CA, USA). Pipette resistance ranged from 0.5 to 1.5 MΩ. The extracellular recording solution was (in mM): 65 NaCl, 85 choline-Cl, 2 $CaCl_2$, and 10 Hepes, titrated to pH 7.4 with TMA-OH (tetramethylammonium hydroxide). After establishing whole-cell conditions, cells were continuously bathed in the extracellular solution with a gravity-fed superfusion system at a rate of approximately 0.1 ml/min. The intracellular (pipette) solution was (in mM): 100 NaF, 30 NaCl, 10 EGTA, and 10 Hepes, titrated to pH 7.2 with CsOH. These solutions create an outward Na^+ gradient and an outward Na^+ current at the test pulse of +50 mV, thus reducing potential problems associated with space clamp or series resistance errors [30]. Series resistance was compensated at 80%. Linear leak subtraction based on five hyperpolarizing pulses was used for all recordings. Any endogenous K^+ currents were blocked with Cs^+ in the pipette, and HEK cells express no native Ca^{2+} current [31]. Cells were selected for recording on the basis of positive immunoreaction with anti-CD8 Dynabeads (Dynal Biotech, Inc., Lake Success, NY, USA). Recordings were performed 1–3 days post-transfection.

The holding potential (V_{hold}) for all experiments was −160 mV. A test pulse to +50 mV (4 ms) was used to record peak available Na^+ current (I_{Na}). Activation curves were obtained from the peak current recorded with pulses from V_{hold} to voltages over the range of −100 mV to +50 mV in 10-mV increments. Steady-state fast inactivation (h_∞) was determined with a test pulse to +50 mV to record I_{Na} following a conditioning prepulse (100 ms) from −160 mV to −30 mV in 10-mV increments. The $V_{1/2}$ and slope factor k of the curves for activation and fast inactivation were obtained from a fit of the data with a Boltzmann function. Three protocols were used to determine slow-inactivation phenotype [18,22,32,33]: (1) *Development of slow inactivation*: voltage was stepped from V_{hold} to 0 mV for various times (10 ms to 60 s), stepped to V_{hold} for 50 ms to allow recovery from fast inactivation, and then stepped to +50 mV (4 ms) to record I_{Na}. I_{Na} was normalized to the initial value recorded before the start of the protocol. Data were fit with a single exponential function. (2) *Recovery from slow inactivation*: voltage was stepped to 0 mV for 60 s, stepped to V_{hold} for various times (50 ms to 30 s), and then a subsequent 4-ms test pulse to +50 mV. I_{Na} was normalized to I_{Na} obtained after 30 s at V_{hold}. Data were fit with a single exponential function. (3) *Voltage dependence of steady-state slow inactivation* (s_∞): we used a 60-s prepulse to voltages from −160 to 0 mV in 20-mV steps, a 50-ms step to V_{hold} (to allow recovery from fast inactivation), and then a 4-ms test pulse to +50 mV to record I_{Na}. I_{Na} was normalized to I_{Na} recorded at V_{hold}. The data were fit with a Boltzmann function.

Application of cysteine modification agent methanethiosulfonate ethylammonium (MTSEA). The cysteine modification agent MTSEA (Toronto Research Chemicals, Toronto, Ontario, Canada) was dissolved in water (15 mM) on the day of the experiment and kept on ice in the dark before final dilution into extracellular solution to 1.5 mM immediately prior to use. MTSEA was applied extracellularly via the gravity-fed superfusion system. We used MTSEA because this compound can access transmembrane protein sites from the extracellular side of the membrane and has previously been used successfully to determine accessibility of pore-lining residues in Navs [18,34,35]. Intracellular application of MTSEA via inclusion in the pipette was also attempted ($n = 3$). However, due to the time necessary for stabilization of whole-cell current recording ($\geqslant$5 min) and the long depolarizations (min) needed to produce slow inactivation in cardiac Navs, this resulted in MTSEA exposure times of >10 min. Long exposure to MTSEA often results in increased holding currents from progressively "leaky" cells, and usually leads to a reduction in current, changes in cell morphology, and loss of electrical recording. This problem may be due to the ability of MTSEA to enter the lipophilic environment of the membrane and possibly disrupt normal membrane function [34].

Cysteine accessibility for MTSEA modification was determined by monitoring effects on whole-cell current with a 4-ms test pulse to +50 mV. For closed-state accessibility the test pulse was from V_{hold} every 10 s. For slow-inactivated state accessibility we used a 60-s prepulse to 0 mV and a 10-s interpulse to V_{hold} (to allow recovery from slow inactivation) before each test pulse. This resulted in a test pulse every 70 s.

Data collection and analysis. Data were collected using an Axopatch 200B amplifier (filtered at 5 kHz) and pCLAMP software (Axon Instruments, Foster City, CA, USA). Analysis of data and curve fits were performed with pCLAMP and Origin software (MICROCAL Software, Inc., Northampton, MA, USA). Differences were considered significant at $p < 0.05$ (ANOVA). Grouped data are presented as means ± SEM.

Results

MTSEA reduces current in wild-type hNav1.5 but not in mutant C373Y

We used whole-cell recording with a 4-ms test pulse from V_{hold} (−160 mV) to +50 mV every 10 s to monitor the baseline effect of 1.5 mM MTSEA on Na^+ current from wild-type hNav1.5. As demonstrated in Figs. 1A and B, MTSEA causes a large, rapid reduction in current recorded from wild-type hNav1.5. Exposure to extracellular MTSEA for 150 s reduced whole-cell current by 80% (Figs. 1A and B). The effect of MTSEA exposure was not reversible with washout, consistent with covalent bonding with a cysteine residue in hNav1.5. The MTSEA-induced reduction in Na^+ current is unique to hNav1.5 because another Nav isoform, hNav1.4 (human skeletal muscle), does not show this response (Fig. 1A). hNav1.4 contains a tyrosine (Y) residue at position 401 in the outer pore region, whereas the homologous site in hNav1.5 contains a cysteine (C373). Substitution of tyrosine (Y) for native cysteine (C) in hNav1.5 at position 373 (C373Y) abolishes the sensitivity of hNav1.5 to MTSEA. Exposure to MTSEA for up to 4 min did not significantly reduce Na^+ current in C373Y (Fig. 1A). Therefore, we used the C373Y mutant as the background for substitution of cysteine (C) for the native valine (V) at position 930 in the D2-S6 double mutant C373Y-V930C.

Fast inactivation and activation in hNav1.5, C373Y, and C373Y-V930C

Measurement of baseline electrophysiological properties showed no significant difference in steady-state fast inactivation with the C373Y and C373Y-V930C mutants when compared with wild-type hNav1.5 (Fig. 2A). The $V_{1/2}$ and k values from the Boltzmann fit for steady-state fast inactivation were, respectively: hNav1.5 ($n = 6$), -80.5 ± 0.5 mV, 8.4 ± 0.4; C373Y ($n = 6$), -74.9 ± 0.4 mV, 6.9 ± 0.4; C373Y-V930C ($n = 11$), -82.9 ± 0.6 mV, 8.2 ± 0.5. The activation (conductance–voltage) curve was left-shifted in C373Y compared with hNav1.5 (Fig. 2B; $p < 0.05$). The $V_{1/2}$ and k values from the Boltzmann fit for activation were, respectively: hNav1.5 ($n = 6$), -43.2 ± 1.0 mV, 10.9 ± 0.9; C373Y ($n = 6$), -51.6 ± 1.2 mV, 9.8 ± 1.0; C373Y-V930C ($n = 11$), -39.8 ± 0.6, 9.1 ± 0.5.

C373Y-V930C is relatively resistant to slow inactivation compared with hNav1.5 and C373Y

Slow-inactivation phenotype was characterized with three protocols which examined development of slow inactivation, recovery from slow inactivation, and steady-state slow inactivation (see Materials and methods). There was no significant difference in slow-inactivation phenotype observed between hNav1.5 and C373Y (Figs. 3A–C). In contrast, C373Y-V930C is somewhat resistant to slow inactivation compared with hNav1.5 and C373Y. After 60 s at 0 mV, C373Y-V930C shows less slow inactivation (≈15%) compared with C373Y and hNav1.5 (≈35–40%; $p < 0.001$; Fig. 3A). In addition, C373Y-V930C recovers faster from slow inactivation with a time constant of 180 ± 40 ms ($p < 0.05$) vs. 420 ± 100 ms for C373Y and 570 ± 100 ms for hNav1.5 (Fig. 3B). Slow inactivation in C373Y-V930C shows less voltage-dependence ($k = 11.6 \pm 1.7$)

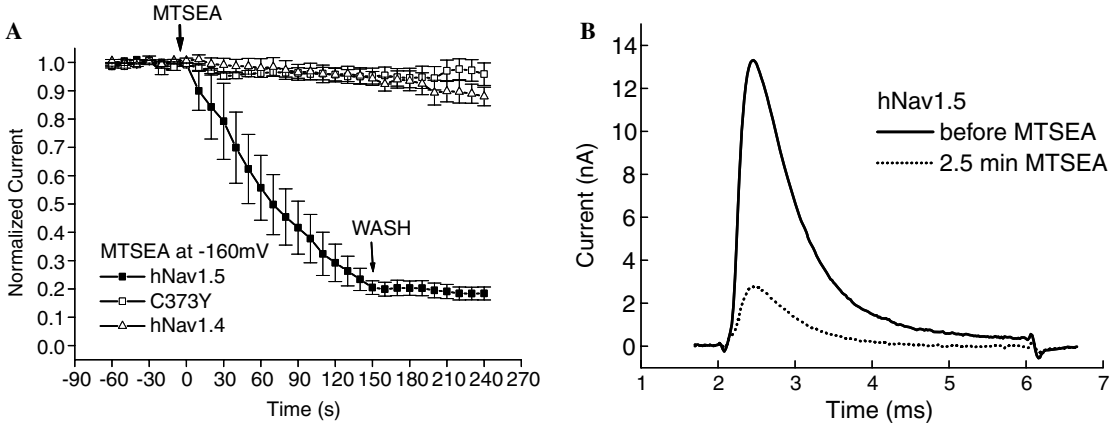

Fig. 1. MTSEA reduces current in wild-type hNav1.5, but not in C373Y or hNav1.4. Current was normalized to recordings prior to 1.5 mM MTSEA application. (A) Grouped data for hNav1.5 ($n = 5$), C373Y ($n = 5$), and hNav1.4 ($n = 4$). Cells were continuously exposed to MTSEA (arrow) for 150 s (hNav1.5) or 240 s (C373Y, hNav1.4). (B) Representative traces from hNav1.5 before MTSEA and after 150 s (2.5 min) exposure to MTSEA.

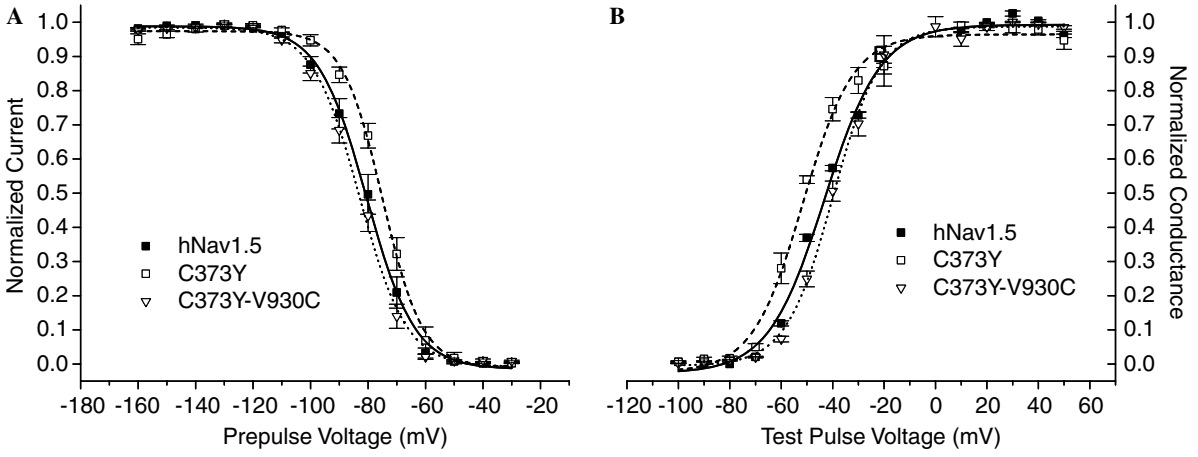

Fig. 2. Steady-state fast inactivation and activation (conductance–voltage) are similar for hNav1.5, C373Y, and C373Y-V930C. Grouped data for hNav1.5 ($n = 6$), C373Y ($n = 6$), and C373Y-V930C ($n = 11$). (A) Steady-state fast inactivation measured with a prepulse of 100 ms from −160 mV to −30 mV in 10-mV increments. (B) Activation curves with test pulses from V_{hold} of −160 mV to −100 mV up to +50 mV in 10-mV increments. Data were fit with the Boltzmann function.

than either hNav1.5 ($k = 18.4 \pm 2.2$; $p < 0.05$) or C373Y ($k = 20.2 \pm 1.8$; $p < 0.001$; Fig. 3C).

MTSEA reduces current in C373Y-V930C in the slow-inactivated state, but not in the fast-inactivated or closed state

To look for state-dependent conformational changes involving residue 930 in D2-S6, we applied 1.5 mM MTSEA to C373Y-V930C in the closed state ($V_{hold} - 160$ mV), the fast-inactivated state, and the slow-inactivated state. When C373Y-V930C was exposed to extracellular MTSEA for 4 min while held at −160 mV (closed state), no significant effect on Na^+ current was observed (Fig. 4). For fast inactivation, depolarization pulses to 0 mV for 100 ms at 5 Hz during 4 min continuous exposure to MTSEA produced no significant effect on current in C373Y-V930C (Fig. 4). Similar results were found using depolarization pulse trains to 0 mV for 4 ms at 50 Hz ($n = 3$; data not shown).

To determine if slow inactivation produces state-dependent molecular rearrangements involving residue 930 in D2-S6, we applied 1.5 mM MTSEA to C373Y-V930C in the slow-inactivated state. We depolarized the cell to 0 mV for 60 s and then allowed recovery from slow inactivation at −160 mV for 10 s prior to the test pulse. We repeated this protocol four times for a total of 4 min of MTSEA exposure at 0 mV. We found that when C373Y-V930C was slow-inactivated during 4 min MTSEA exposure, there was a significant decrease in Na^+ current to about 50% of baseline ($p < 0.001$ compared with C373Y; Fig. 5). This effect was not reversed by post-MTSEA washing (Fig. 5).

We also studied the slow-inactivation-induced accessibility change in C373Y-V930C with another MTS compound, methanethiosulfonate ethyltrimethylammonium (MTSET), both extracellularly and intracellularly. We found no effect on slow inactivated channels with extracellular application of 1 mM MTSET ($n = 3$) or intracellular MTSET ($n = 4$; data not shown).

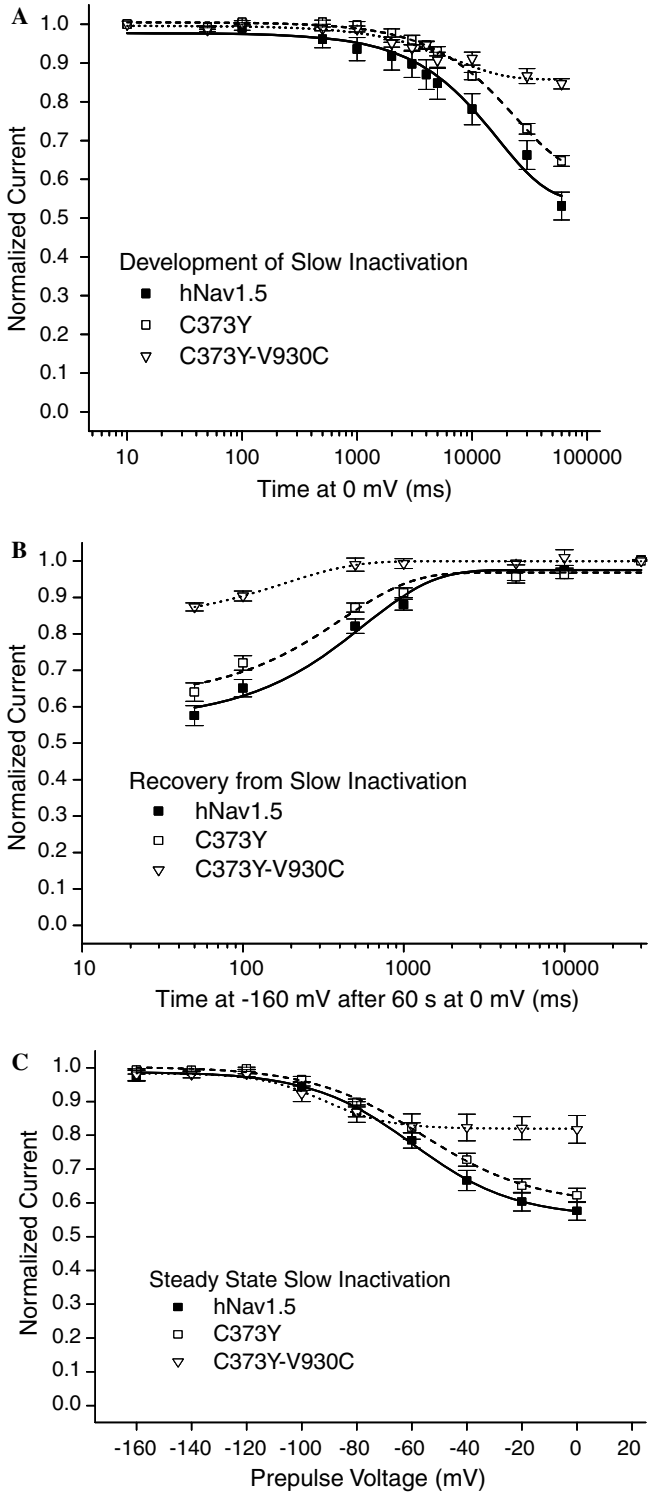

Fig. 3. Slow inactivation phenotype shown as development of, recovery from, and steady-state slow inactivation. Wild-type hNav1.5 and C373Y are comparable in slow-inactivation phenotype. In contrast, C373Y-V930C is relatively resistant to slow inactivation compared with hNav1.5 and C373Y. (A) After 60 s at 0 mV, hNav1.5 ($n = 7$) and C373Y ($n = 5$) are ≈35–40% slow-inactivated, while C373Y-V930C ($n = 14$) is ≈15% slow-inactivated at this time ($p < 0.001$). (B) Navs recover from slow inactivation by 10 s of repolarization to V_{hold} (−160 mV) with C373Y-V930C ($n = 9$) recovering faster (by 1 s) than either hNav1.5 ($n = 8$) or C373Y ($n = 7$). (C) Slow inactivation in C373Y-V930C shows less voltage-dependence ($n = 6$) than either hNav1.5 ($p < 0.05$; $n = 10$) or C373Y ($p < 0.001$; $n = 12$).

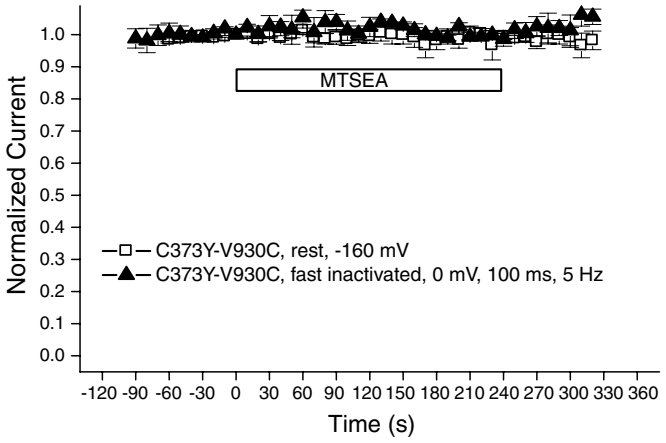

Fig. 4. MTSEA (1.5 mM) application for 4 min (240 s) starting at time 0 to C373Y-V930C at rest ($n = 3$) or in the fast-inactivated state ($n = 3$) does not significantly reduce current. Fast inactivation was produced using depolarization pulses to 0 mV for 100 ms at 5 Hz from V_{hold} of −160 mV. A 4-ms test pulse to +50 mV was applied every 10 s.

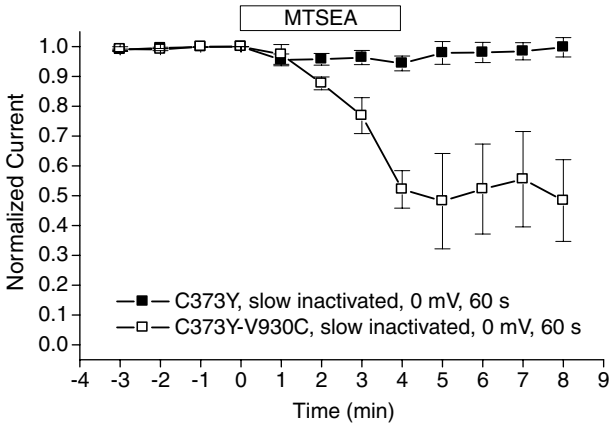

Fig. 5. C373Y-V930C is modified by MTSEA only when in the slow-inactivated state. Cells were continuously exposed to 1.5 mM MTSEA for 4 min starting at time 0. After 60 s depolarization at 0 mV, the cells were stepped to −160 mV for 10 s to allow recovery from slow inactivation and then pulsed to +50 mV. (Note: the graph does not include the 10 s interpulse, so the abscissa indicates the time that the cells were exposed to MTSEA while being held at 0 mV). A significant decrease in current after MTSEA exposure is seen with C373Y-V930C ($n = 6$; $p < 0.001$ at 4 min) but not C373Y ($n = 7$).

Discussion

Slow inactivation in Navs can play an important role in normal physiological function of excitable tissues. In this study, we examined molecular mechanisms underlying the process of slow inactivation in cardiac Navs. Specifically, we wanted to determine if slow inactivation induces conformational changes impacting transmembrane segment 6 of domain 2 (D2-S6) in human cardiac Na^+ channel hNav1.5. Using cysteine substitution and MTSEA-accessibility, we found that residue 930 in D2-S6 is inaccessible to MTSEA-modification in the closed state (−160 mV), but becomes accessible to modification in the slow-inactivated state (0 mV).

MTSEA effects on current in wild-type hNav1.5 and mutant C373Y

In order to use the substituted-cysteine accessibility method (SCAM) [24], there must be no response to application of MTSEA with the wild-type hNav1.5 control. However, this is not the case for hNav1.5, in which short application of MTSEA produces large and rapid decreases in Na^+ current recorded. This effect is non-reversible during extended periods of wash after MTSEA application, suggesting that there is covalent reactivity between a native cysteine and MTSEA. This is not surprising because the rat cardiac Na^+ channel rNav1.5 also shows this response [25]. To eliminate MTSEA reactivity in wild-type hNav1.5, we substituted tyrosine (Y) for the native cysteine (C) in the mutant C373Y. We chose tyrosine because this is the homologous residue in human skeletal muscle hNav1.4, an isoform that does not respond to MTSEA. We then used the hNav1.5 mutant C373Y, which does not show a response to MTSEA, as the baseline for our study.

Activation and fast inactivation in hNav1.5, C373Y, and C373Y-V930C

We substituted cysteine at V930 in the hNav1.5 mutant C373Y to produce the mutant C373Y-V930C. We chose the V930 site because we have previously demonstrated state-dependent MTSEA-accessibility at the homologous site, V787 in D2-S6, in rat skeletal muscle rNav1.4 [18] and we were interested in determining if the cardiac hNav1.5 shared similar molecular mechanisms of slow inactivation. The only significant difference in activation and steady-state fast inactivation between the mutants and wild-type was a hyperpolarizing shift of about 9 mV in the activation (conductance–voltage) curve of C373Y compared with hNav1.5. These results demonstrate that the substitutions do not dramatically disrupt normal fast gating.

Slow inactivation in hNav1.5, C373Y, and C373Y-V930C

We found that substitution of tyrosine in C373Y did not affect slow inactivation compared with hNav1.5. However, substitution of cysteine at V930 in C373Y-V930C produces a relative resistance to entry into and a more rapid recovery from slow inactivation compared with hNav1.5 and C373Y. In addition, steady-state slow inactivation in C373Y-V930C is less sensitive to changes in voltage compared with the other channels. These data suggest that position 930, located in the inner pore region [17], may be an important molecular determinant for slow inactivation in hNav1.5. This conclusion is supported by our previous study showing that the homologous mutant V787C in the rNav1.4 background also confers some resistance to slow inactivation [18].

This observation also lends support to the proposal that cardiac Nav1.5 and skeletal muscle Nav1.4 share some related molecular mechanisms of slow inactivation. This is an interesting result because the two isoforms exhibit dramatically different overall slow-inactivation phenotypes, with Nav1.5 being more resistant to slow inactivation compared with Nav1.4 [22,23]. While the molecular mechanisms that make Nav1.5 more resistant to slow inactivation than Nav1.4 are not known, the results from this study suggest a role for the S6 segments in this process. Future experiments with additional substitutions in D2-S6 and substitutions in the other domains (D1, D3, and D4) should provide further information on the interaction of the S6 segments during prolonged depolarizations in Navs.

MTSEA effects on C373Y-V930C in the slow-inactivated state compared with the closed state

Our main interest in this study was the state-dependent accessibility of substituted cysteines to MTS agents as a function of state-dependent conformational changes. We used MTSEA because this compound can readily enter the membrane from either side and can access sites deep within the protein [34]. This characteristic of MTSEA has been successfully exploited to determine accessibility of pore-lining and other residues in Navs [18,34,35]. This contrasts with other MTS reagents which do not readily enter the membrane, e.g., methanethiosulfonate ethyltrimethylammonium (MTSET), but which are quite effective when cysteine residues are closer to the intracellular or extracellular side of Navs [36–38]. Therefore, MTSET may not produce a functional effect in Navs in situations where MTSEA shows an effect [18]. This may be due to inaccessibility of the pore to these reagents because of occlusion by the fast inactivation gate on the intracellular side and restricted access due to the selectivity filter at the extracellular side.

When MTSEA is applied to C373Y-V930C at −160 mV (closed state), there is no significant effect on Na^+ current. Also, there is no effect on Na^+ current with protocols using short depolarizations that produce fast inactivation in C373Y-V930C. However, when C373Y-V930C is slow-inactivated at 0 mV in the presence of MTSEA, there is a marked decrease in Na^+ current. We propose that the difference in response to MTSEA is due to a change in accessibility of 930C to MTSEA during slow inactivation. We suggest that 930C is inaccessible in the closed and fast-inactivated states, e.g., buried in the protein or facing away from the pore, but becomes accessible to MTSEA when in the slow-inactivated state, e.g., facing the pore. This conclusion is consistent with other studies demonstrating slow-inactivation-dependent molecular rearrangement in Navs [18,39]. For example, previously we demonstrated that in the rNav1.4 mutant V787C, MTSEA reduces current when applied in the slow-inactivated state, but not when applied at rest [18]. Conversely, Vedantham and Cannon [39] found that application of MTSEA in the rNav1.4 mutant V1583C (cysteine substituted for valine in D4-S6) reduced current at rest, but not in the slow-inactivated state. Although

the mechanism of Na^+ current reduction by MTSEA is unknown, it may be due to steric hindrance or conformational changes that result in disruption of normal voltage gating, or to a direct physical blocking of Na^+ ion flow through the pore.

The accessibility of 930C to modification by MTSEA was observed in the mutant C373Y-V930C, which is relatively resistant to slow inactivation compared with wild-type hNav1.5. Therefore, the accessibility of 930C in this mutant may differ from that of the native V930 found in wild-type hNav1.5. However, C373Y-V930C expresses well, shows no obvious disruption in fast gating, and exhibits a definite slow-inactivation phenotype. Thus, the difference in slow inactivation between hNav1.5 and C373Y-V930C does not appear to represent a major disruption of molecular structure or the slow-inactivation gating process. Interestingly, an earlier study demonstrated a similar moderate resistance to slow inactivation with alanine substitution at the homologous site in the rNav1.4 isoform mutant V787A [18].

In conclusion, we have demonstrated that slow inactivation in C373Y-V930C changes the position of the 930C residue as monitored by MTSEA accessibility. Taken together with previous results implicating S6 segments in slow inactivation [18,19,39], we propose that this change in MTSEA accessibility during prolonged depolarization is due to a change in the relative position of D2-S6 within the inner pore region. Although Nav slow inactivation is a complex process that likely involves different domains of the protein, our current data support the hypothesis that slow-inactivation gating in hNav1.5 (and perhaps other Nav isoforms) involves conformational changes in the inner pore region of D2-S6.

Acknowledgments

The authors thank Dr. Theodore R. Cummins, Indiana University School of Medicine, Indianapolis, IN, USA, for the hNav1.4 and hNav1.5 clones. This work was supported by Faculty Development Grants from Southeastern Louisiana University and by National Heart, Lung, and Blood Institute Grant R15 HL080009-01 to JOR.

References

[1] M. Noda, T. Ikeda, H. Suzuki, H. Takeshima, T. Takahashi, M. Kuno, S. Numa, Expression of functional sodium channels from cloned cDNA, Nature 322 (1986) 826–828.
[2] J.S. Trimmer, S.S. Cooperman, S.A. Tomiko, J.Y. Zhou, S.M. Crean, M.B. Boyle, R.G. Kallen, Z.H. Sheng, R.L. Barchi, F.J. Sigworth, Primary structure and functional expression of a mammalian skeletal muscle sodium channel, Neuron 3 (1989) 33–49.
[3] M.E. Gellens, A.L.J. George, L.-Q. Chen, M. Chahine, R. Horn, R.L. Barchi, R.G. Kallen, Primary structure and functional expression of the human cardiac tetrodotoxin-insensitive voltage-dependent sodium channel, Proc. Natl. Acad. Sci. USA 89 (1992) 554–558.
[4] A.L. Hodgkin, A.E. Huxley, A quantitative description of membrane current and its application to conduction and excitation in nerve, J. Physiol. (London) 117 (1952) 500–544.
[5] R.L. Ruff, L. Simoncini, W. Stuhmer, Slow sodium channel inactivation in mammalian muscle: a possible role in regulating excitability, Muscle Nerve 11 (1988) 502–510.
[6] A. Sawczuk, R.K. Powers, M.D. Binder, Spike frequency adaptation studied in hypoglossal motorneurons of the rat, J. Neurophysiol. 73 (1995) 1799–1810.
[7] B. Rudy, Slow inactivation of the sodium conductance in squid giant axons. Pronase resistance, J. Physiol. (London) 283 (1978) 1–21.
[8] D.E. Featherstone, J.E. Richmond, P.C. Ruben, Interaction between fast and slow inactivation in Skm1 sodium channels, Biophys. J. 71 (1996) 3098–3109.
[9] R.S. Kass, The channelopathies: novel insights into molecular and genetic mechanisms of human disease, J. Clin. Invest. 115 (2005) 1986–1989.
[10] M.H. Meisler, J.A. Kearney, Sodium channel mutations in epilepsy and other neurological disorders, J. Clin. Invest. 115 (2005) 2010–2017.
[11] K. Jurkat-Rott, F. Lehmann-Horn, Muscle channelopathies and critical points in functional and genetic studies, J. Clin. Invest. 115 (2005) 2000–2009.
[12] A.J. Moss, R.S. Kass, Long QT syndrome: from channels to cardiac arrhythmias, J. Clin. Invest. 115 (2005) 2018–2024.
[13] A.L. George, Inherited disorders of voltage-gated sodium channels, J. Clin. Invest. 115 (2005) 1990–1999.
[14] W. Stuhmer, F. Conti, H. Suzuki, X.D. Wang, M. Noda, N. Yahagi, H. Kubo, S. Numa, Structural parts involved in activation and inactivation of the sodium channel, Nature 339 (1989) 597–603.
[15] D.E. Patton, J.W. West, W.A. Catterall, A.L. Goldin, Amino acid residues required for fast Na^+-channel inactivation: charge neutralizations and deletions in the III–IV linker, Proc. Natl. Acad. Sci.USA 89 (1992) 10905–10909.
[16] G. Yellen, D. Sodickson, T.Y. Chen, M.E. Jurman, An engineered cysteine in the external mouth of a K^+ channel allows inactivation to be modulated by metal binding, Biophys. J. 66 (1994) 1068–1075.
[17] G.M. Lipkind, H.A. Fozzard, KcsA crystal structure as framework for a molecular model of the Na(+) channel pore, Biochemistry 39 (2000) 8161–8170.
[18] J.P. O'Reilly, S.Y. Wang, G.K. Wang, Residue-specific effects on slow inactivation at V787 in D2-S6 of Na(v)1.4 sodium channels, Biophys. J. 81 (2001) 2100–2111.
[19] S.-Y. Wang, G.K. Wang, A mutation in segment I-S6 alters slow inactivation of sodium channels, Biophys. J. 72 (1997) 1633–1640.
[20] L.J. Hayward, R.H.J. Brown, S.C. Cannon, Slow inactivation differs among mutant Na channels associated with myotonia and periodic paralysis, Biophys. J. 72 (1997) 1204–1219.
[21] M.P. Takahashi, S.C. Cannon, Enhanced slow inactivation by V445M: a sodium channel mutation associated with myotonia, Biophys. J. 76 (1999) 861–868.
[22] J.P. O'Reilly, S.-Y. Wang, R.G. Kallen, G.K. Wang, Comparison of slow inactivation in human heart and rat skeletal muscle Na channel chimeras, J. Physiol. (London) 515.1 (1999) 61–73.
[23] J.E. Richmond, D.E. Featherstone, H.A. Hartmann, P.C. Ruben, Slow inactivation in human cardiac sodium channels, Biophys. J. 74 (1998) 2945–2952.
[24] A. Karlin, M.H. Akabas, Substituted-cysteine accessibility method, Methods Enzymol. 293 (1998) 123–145.
[25] G.E. Kirsch, M. Alam, H.A. Hartmann, Differential effects of sulfhydryl reagents on saxitoxin and tetrodotoxin block of voltage-dependent Na channels, Biophys. J. 67 (1994) 2305–2315.
[26] W. Wang, B.A. Malcolm, Two-stage polymerase chain reaction protocol allowing introduction of multiple mutations, deletions, and insertions, using QuikChange site-directed mutagenesis, Methods Mol. Biol. 182 (2002) 37–43.
[27] W. Wang, B.A. Malcolm, Two-stage PCR protocol allowing introduction of multiple mutations, deletions and insertions using QuikChange Site-Directed Mutagenesis, Biotechniques 26 (1999) 680–682.

[28] F.L. Graham, A.J. Eb, A new technique for the assay of infectivity of human adenovirus 5 DNA, Virology 52 (1973) 456–467.
[29] O.P. Hamill, A. Marty, E. Neher, B. Sakmann, F.J. Sigworth, Improved patch-clamp techniques for high-resolution current recording from cells and cell-free membrane patches, Pflugers Arch. 391 (1981) 85–100.
[30] G. Cota, C.M. Armstrong, Sodium channel gating in clonal pituitary cells. The inactivation step is not voltage dependent, J. Gen. Physiol. 94 (1989) 213–232.
[31] C. Ukomadu, J. Zhou, F.J. Sigworth, W.S. Agnew, mI Na^+ channels expressed transiently in human embryonic kidney cells: biochemical and biophysical properties, Neuron 8 (1992) 663–676.
[32] J.P. O'Reilly, S.Y. Wang, G.K. Wang, Methanethiosulfonate-modification alters local anesthetic block in rNav1.4 cysteine-substituted mutants S1276C and L1280C, J. Membr. Biol. 193 (2003) 47–55.
[33] J.P. O'Reilly, S.Y. Wang, G.K. Wang, A point mutation in domain 4-segment 6 of the skeletal muscle sodium channel produces an atypical inactivation state, Biophys. J. 78 (2000) 773–784.
[34] M. Holmgren, Y. Liu, Y. Xu, G. Yellen, On the use of thiol-modifying agents to determine channel topology, Neuropharmacology 35 (1996) 797–804.
[35] A. Sunami, A. Tracey, I.W. Glaaser, G.M. Lipkind, D.A. Hanck, H.A. Fozzard, Accessibility of mid-segment domain IV S6 residues of the voltage-gated Na^+ channel to methanethiosulfonate reagents, J. Physiol. 561 (2004) 403–413.
[36] I. Deschenes, E. Trottier, M. Chahine, Cysteine scanning analysis of the IFM cluster in the inactivation gate of a human heart sodium channel, Cardiovasc. Res. 42 (1999) 521–529.
[37] A.F. Struyk, S.C. Cannon, Slow inactivation does not block the aqueous accessibility to the outer pore of voltage-gated Na channels, J. Gen. Physiol. 120 (2002) 509–516.
[38] N. Yang, A.L.J. George, R. Horn, Probing the outer vestibule of a sodium channel voltage sensor, Biophys. J. 73 (1997) 2260–2268.
[39] V. Vedantham, S.C. Cannon, Rapid and slow voltage-dependent conformational changes in segment IVS6 of voltage-gated Na(+) channels, Biophys. J. 78 (2000) 2943–2958.